Analysis and Design for the moderately deep postbuckling behaviour of composite plates

Zhangming Wu[1]
Cardiff University, Cardiff, Wales CF24 3AA, United Kingdom

Tongji University, Shanghai 200092, People's Republic of China.

Gangadharan Raju[2]
Indian Institute of Technology Hyderabad, Telangana 502285, India

Paul Weaver[3]
University of Bristol, Bristol, England BS8 1TR, United Kingdom

It is widely acknowledged that tracking the postbuckling response of structures made from thin plates can be problematical. Such difficulty is associated with highly nonlinear effects including mode jumping, imperfection sensitivity and their combined interactions. Two widely used techniques that are currently used involve path following and asymptotic expansion. The former is often implemented in commercial finite element codes but can prove unreliable at representing branch switching. The latter is a relatively quick technique due to its recursive linear nature but is only reliable in the vicinity of bifurcations. Due to the overall complex nonlinearity, analytical closed form solutions do not exist for path following and rarely for quadratic asymptotic expansions where simple forms have been adopted. This paper presents an analytical-based approach that enables the efficient optimal design of "moderately deep" nonlinear postbuckling behaviour of laminated composite plates under uniaxial or biaxial loading. It provides a closed form solution that more reliably reflects deeper postbuckling response than the state-of-the-art. Subsequently, highly efficient

---

[1] Lecturer, Cardiff School of Engineering, Queen's Buildings, The Parade, Cardiff CF24 3AA, United Kingdom
[2] Assistant professor, Dept of Mechanical and Aerospace Engineering, IIT Hyderabad
[3] Professor in Lightweight Structures, Advanced Composite Centre for Innovation and Science, Department of Aerospace Engineering, Queen's Building, University Walk.

postbuckling optimization is attributed to the newly derived closed-form solution and a recent two-level optimization framework.

I. Introduction

Laminated composite plates are increasingly used in primary aerospace structures. In the current design philosophy buckling is confined to the ultimate load state, however, it is well-known that plates, unlike many beams and shells, may load further in excess of their critical buckling load before the occurrence of final failure. An alternate philosophy could be one in which buckling is allowed to occur at loads closer to the limit state, thus reducing the number of plies in the laminates. One problem with this concept is the added complications of non-linearity, caused by transverse deflections, and the associated difficulty it would bring to the design process. Today, solutions for such problems may be computed routinely with commercial finite-element codes, however, the computational requirements of such models (albeit relatively small by current modelling standards) are far in excess of what is practical in large-scale structural optimization problems.

Over the last two decades, relatively little work has been conducted to optimize the postbuckling behaviour of composite structures [1–16]. Optimal design of composite structures for postbuckling performance based on finite element methods (FEM) generally encounter high computational cost difficulties. Therefore, early efforts were made to develop mathematical models that can rapidly determine the postbuckling strength of composite structures, including use of the closed-form expressions [1, 3], Rayleigh-Ritz method [2, 6], Galerkin method [4], (Koiter's) perturbation method [1, 3, 5] and the finite strip method [15, 16]. Applying these efficient models into optimization routines, a few specialized tools for the postbuckling optimization of composite structures have been implemented, such as POSTOP [1], PANDA2 [3], NLPANOPT [5, 14] and VICONOPT [15, 16]. To overcome the computational problems, an alternative strategy of constructing approximate models (also known as surrogate models or response surface models) to replace the expensive FEM simulation in the optimization process has been extensively used in recent years. A number of methods have been successfully applied to build the global/local approximation models for postbuckling anal-

ysis of composite structures, for example, the polynomial regression function [8], Artificial Neural Networks [9, 10], Radial Basis Functions [10] and Kriging method [9]. The minimum weight design of composite structural components (stiffened panels and shells) considering their postbuckling response was carried out using these tools or approximate models. However, these specific codes received limited applications and further development by other researchers partially due to their exclusivity. The development of a completely analytical method that explicitly give the postbuckling solutions (in closed-form) for the optimal design of postbuckling behaviour of composite structures, therefore, remains of significant interests.

Based on von Kármán's expressions, numerous works of analytical or semi-analytical methods have been proposed to study the postbuckling behaviour of plates. Early works developed closed-form solutions for isotropic plates [17–21]. Harris [22] proposed a closed-form expression for determining the initial postbuckling stiffness of orthotropic composite plates. As an alternative method to directly solve the governing equation or the energy function, perturbation methods provide an effective way to solve the nonlinear problem asymptotically. Stein [21] proposed a perturbation model for the postbuckling analysis of isotropic plates. Later, Chandra and Raju [23] extended Stein's model for orthotropic plates. Shen and Zhang [30] originally employed the Airy's stress function and perturbation method to derive the closed-form asymptotic postbuckling solutions for isotropic plates under biaxial compression. They later extended this method in the derivation of the closed-form asymptotic solutions for orthortropic plates [24]. However, in all of these models the accuracy of the solutions was not retained at loads much beyond the buckling load, especially in the case of highly orthotropic laminates. In the current work, an analytical model, based on an improvement of Zhang and Shen's work [24], is developed giving explicit closed-form formula for both the end-shortening strain and maximum transverse deflection in terms of the boundary stress resultants and material stiffnesses. The closed-form postbuckling model also enables designers to take advantage of recent developments in structural optimization methods. The improved accuracy of this new postbuckling solution is mainly due to the selection of an alternative choice of perturbation parameter and a different way of truncating the high-order terms. The new formulation is capable of capturing moderately deep post-buckling behaviour. The terminology "moderately deep

postbuckling" used here describes a postbuckled plate with significant nonlinear behaviour. This behaviour is in contrast to the commonly used initial postbuckling response which essentially uses a linear model with reduced stiffness or effective-width [17, 22]. The deep postbuckling behaviour requires more nonlinear terms in the modelling process to capture the plate deformation or stress resultants.

The optimization process for the postbuckling behaviour design of composite laminated plates is conducted in a two-level strategy using lamination parameters as intermediate design variables [25]. Diaconu and Weaver [26] derived the closed-form solution for the initial postbuckling response of infinitely long and symmetrically laminated composite plates, and applied it into a two-level strategy for the postbuckling optimization. The closed-form postbuckling solution derived currently is suitable for the design of finite-length composite plates. In addition, it is also able to capture the moderately deep postbuckling behaviour. In the first step, orthotropic composite plates are defined in terms of four lamination parameters ($\xi_{1,2}^{A,D}$). A gradient-based mathematical programming algorithm (Globally Convergent Method of Moving Asymptotes - GCMMA) is applied to determine the lamination parameters, which minimize either the end-shortening strain or the maximum transverse deflection. In the second step, optimal layups are computed from the obtained lamination parameters using a genetic algorithm (GA). Numerical examples are investigated based on the simply-supported plate with different aspect ratios and in-plane loading cases.

II. Postbuckling Analysis

A. Basic equations

In classical lamination plate theory (CLPT), the constitutive equations for rectangular composite plates in a partially inverted form is defined as [27],

$$\begin{pmatrix} \epsilon^0 \\ \mathbf{M} \end{pmatrix} = \begin{bmatrix} \mathbf{a} & \mathbf{b} \\ -\mathbf{b^T} & \mathbf{D}^* \end{bmatrix} \begin{pmatrix} \mathbf{N} \\ \kappa \end{pmatrix} \tag{1}$$

where $\mathbf{a} = \mathbf{A^{-1}}$, $\mathbf{b} = -\mathbf{A^{-1}B}$, $\mathbf{D}^* = \mathbf{D} - \mathbf{BA^{-1}B}$ and $\mathbf{A}$, $\mathbf{B}$ and $\mathbf{D}$ are in-plane, coupling and bending stiffness matrices, respectively. The term ϵ^0 is the mid-plane strain, κ is the curvature and $\mathbf{N}$, and $\mathbf{M}$ are in-plane stress and bending moment resultants, respectively. The composite plates

studied in this paper are orthotropic, that is $\mathbf{B} = 0$ and $\mathbf{D}^* = \mathbf{D}$.

The von Kármán large deflection equations that define the nonlinear relation between the mid-plane strains and mid-plane displacements are [28],

$$\epsilon_x^0 = u_{,x}^0 + \tfrac{1}{2}w_{,x}^2 \quad \epsilon_y^0 = v_{,y}^0 + \tfrac{1}{2}w_{,y}^2 \quad \epsilon_{xy}^0 = u_{,y}^0 + v_{,x}^0 + w_{,x}w_{,y} \tag{2}$$

The in-plane stretching behaviour of a plate is modelled by the Airy's stress function(Φ) in our model, The stress resultants $\mathbf{N}$ (N_x, N_y, N_{xy}) are defined as,

$$N_x = \Phi_{,yy}, \quad N_y = \Phi_{,xx}, \quad N_{xy} = -\Phi_{,xy} \tag{3}$$

On the basis of Eqs.(1), (2) and (3), we write the compatibility and equilibrium equations for a plate with large transverse displacements as[26, 29]

$$\begin{aligned} &a_{11}\Phi_{,yyyy} + (2a_{12} + a_{66})\Phi_{,xxyy} + a_{22}\Phi_{,xxxx} \\ &- 2a_{16}\Phi_{,xyyy} - 2a_{26}\Phi_{,xxxy} = (w_{,xy})^2 - (w_{,xx})(w_{,yy}) \end{aligned} \tag{4}$$

$$\begin{aligned} &D_{11}w_{,xxxx} + 2(D_{12} + 2D_{66})w_{,xxyy} + D_{12}w_{,yy} + D_{22}w_{,yyyy} + \\ &4D_{16}w_{,xxxy} + 4D_{26}w_{,xyyy} + \Phi_{,yy}w_{,xx} + \Phi_{,xx}w_{,yy} - 2\Phi_{,xy}w_{,xy} = 0 \end{aligned} \tag{5}$$

Confining the analysis to orthotropic laminates, that is $a_{16} = a_{26} = 0$ and $D_{16} = D_{26} = 0$, the problematic anisotropic terms in Eqs. (4) and (5) are eliminated.

B. Asymptotic solutions

The closed-form asymptotic solutions for the postbuckling analysis of constant stiffness plates are derived with a perturbation analysis [21, 30]. As illustrated in Figure 1, the laminated plate studied in this paper is simply-supported and subjected to a biaxial loading. The ratio between the longitudinal loading (N_{x0}) and transverse loading (N_{y0}) is denoted by k. The four edges are assumed to remain straight during the loading and deformation, that are constant in-plane displacement boundary conditions,

$$u_{,y}(0, y) = u_{,y}(a, y) = v_{,x}(x, 0) = v_{,x}(x, b) = 0. \tag{6}$$

To satisfy the boundary conditions and also consider nonlinear structural behaviour in post-buckling regime, the out-of-plane deflection and Airy's stress function are expressed in the following perturbation forms [21, 24, 30],

$$\begin{aligned} w(x,y) =& \varepsilon \left[w_1 \sin\frac{m\pi x}{a} \sin\frac{n\pi y}{b} \right] + \varepsilon^3 \left[w_3 \sin\frac{m\pi x}{a} \sin\frac{n\pi y}{b} + \right. \\ & \left. w_{13} \sin\frac{m\pi x}{a} \sin\frac{3n\pi y}{b} + w_{31} \sin\frac{3m\pi x}{a} \sin\frac{n\pi y}{b} \right] + \mathcal{O}(\varepsilon^5) \end{aligned} \tag{7}$$

$$\begin{aligned} \Phi(x,y) =& -\phi_x^{(0)} \frac{y^2}{2} - \phi_y^{(0)} \frac{x^2}{2} + \varepsilon^2 \left[-\phi_x^{(2)} \frac{y^2}{2} - \phi_y^{(2)} \frac{x^2}{2} + \right. \\ & \left. \phi_{20}^{(2)} \cos\frac{2m\pi x}{a} + \phi_{02}^{(2)} \cos\frac{2n\pi y}{b} \right] + \varepsilon^4 \left[-\phi_x^{(4)} \frac{y^2}{2} - \phi_y^{(4)} \frac{x^2}{2} + \right. \\ & \phi_{20}^{(4)} \cos\frac{2m\pi x}{a} + \phi_{02}^{(4)} \cos\frac{2n\pi y}{b} + \phi_{22}^{(4)} \cos\frac{2m\pi x}{a} \cos\frac{2n\pi y}{b} + \\ & \phi_{40}^{(4)} \cos\frac{4m\pi x}{a} + \phi_{04}^{(4)} \cos\frac{4n\pi y}{b} + \phi_{24}^{(4)} \cos\frac{2m\pi x}{a} \cos\frac{4n\pi y}{b} + \\ & \left. \phi_{42}^{(4)} \cos\frac{4m\pi x}{a} \cos\frac{2n\pi y}{b} \right] + \mathcal{O}(\varepsilon^6) \end{aligned} \tag{8}$$

where m and n are the number of half-waves of w in x and y directions, respectively. Note, the zeroth, second and fourth order terms of out-of-plane displacement (w) and first and third order terms of Airy function (Φ) are eliminated due to the orthogonality condition [38]. Substituting the expressions of (7) and (8) into the postbuckling governing equations (4) and (5) results in a set of linear non-homogeneous equations, where the unknown coefficients $(w_1, w_3, \cdots, \phi_{20}^{(2)}, \cdots)$ can be determined by a step-by-step procedure [21, 24, 30]. The difference between Zhang and Shen's model [24] and the present work is the assumption for truncating the higher order terms $(\mathcal{O}(\varepsilon^5), \mathcal{O}(\varepsilon^6), \cdots)$ in the derivation of closed-form expressions of these unknown coefficients and the choice of perturbation parameter ε. In Zhang and Shen's model, the coefficient w_3 is assumed to be 0 and the perturbation parameter is chosen by truncating the expansion of the maximum transverse deflection. In our work, the perturbation parameter is chosen from the in-plane stress resultant in the x-direction at the boundary N_{x0}. We have found that retaining more terms for mode shape assumption (Eq. 7) is beneficial to accurately capture the nonlinearity of postbuckling behaviour of composite laminates in "moderately deep" range. As such, it is necessary to include the coefficient w_3 in the derivation of postbuckling solution. The importance of coefficient w_3 will be demonstrated in the subsequent comparison with Zhang and Shen's model. The in-plane stress

resultant N_{x0} is given by the following series,

$$N_{x0} = N_x^{(0)} + \varepsilon^2 N_x^{(2)} + \varepsilon^4 N_x^{(4)} + \cdots \tag{9}$$

where each component of the series expansion for N_{x0} is related to the coefficients in Eq. (8) by the relations $N_x^{(0)} = \phi_x^{(0)}$, $N_x^{(2)} = \phi_x^{(2)}$, $N_x^{(4)} = \phi_x^{(4)}$. In Eq. (9), the term $\varepsilon^4 N_x^{(4)}$ and higher order perturbation terms are ignored ($N_x^{(4)} = 0 \cdots$). The perturbation parameter then becomes [21, 23],

$$\varepsilon^2 = \frac{N_{x0} - N_x^{(0)}}{N_x^{(2)}} \tag{10}$$

The unknown coefficients in Eqs. (7) and (8) are determined as,

$$\phi_x^{(0)} = N_x^{cr} = \left(\frac{m\pi}{a}\right)^2 \frac{\left[D_{11} + 2(D_{12} + 2D_{66})\alpha^2 + D_{22}\alpha^4\right]}{1 + k\alpha^2} \tag{11}$$

$$\phi_{02}^{(2)} = \frac{w_1^2}{32 a_{11}\alpha^2}, \quad \phi_{20}^{(2)} = \frac{\alpha^2 w_1^2}{32 a_{22}} \tag{12}$$

$$\phi_x^{(2)} = \frac{w_1^2}{16(1 + k\alpha^2)} \left(\frac{n\pi}{b}\right)^2 \left(\frac{1}{a_{11}\alpha^2} + \frac{\alpha^2}{a_{22}}\right) \tag{13}$$

$$\begin{aligned} w_{13} &= \frac{(1 + k\alpha^2) w_1^3}{(16 a_{11}\alpha^2)[-8kD_{11} + 16(D_{12} + 2D_{66}) + (80 - 72k\alpha^2) D_{22}\alpha^2]} \\ w_{31} &= \frac{\alpha^4 (1 + k\alpha^2) w_1^3}{(16 a_{22})[(72 - 80k\alpha^2) D_{11} + 16k\alpha^4 (D_{12} + 2D_{66}) - 8D_{22}\alpha^4]} \end{aligned} \tag{14}$$

$$w_3 = \frac{3}{2} \frac{\phi_{02}^{(2)} w_{13} + \phi_{20}^{(2)} w_{31}}{\phi_{02}^{(2)} + \phi_{20}^{(2)}} w_1^3 \tag{15}$$

where $k = N_{x0}/N_{y0}$ is the specified loading ratio, N_x^{cr} is the critical buckling load of plate and $\alpha = na/mb$ is the buckling mode parameter.

For a uniaxial compression-loaded plate, the number of half-waves along the x and y directions are given by,

$$m = (a/b) \sqrt[4]{D_{22}/D_{11}} \quad n = 1. \tag{16}$$

where $(a/b)\sqrt[4]{D_{22}/D_{11}}$ is also known as the effective aspect ratio.

For the case of biaxial compressive loading, however, no formulae exists for the number of half-waves (m and n) that can directly determine the lowest buckling load in Eq. (11). Libove [31] proved that, when a simply-supported orthotropic plate in biaxial compression buckles, one of the number of half waves in the principle directions, m or n, must be one. Tung *et al.* [32] further studied this problem and gave the formula to determine m and n for different cases, which are classified by the effective aspect ratio (α) and the specified loading ratio (k).

The number of half-waves m and n that give the lowest buckling load of a plate under biaxial compression can be determined through analysing the stationary points of Eq. (11). From Libove's proof, the minimum value of N_x^{cr} in Eq. (11) only occurs when either m or n equals to 1. Let $n = 1$, the stationary condition of Eq. (11) results in a quadratic equation with respect to m^2. The following expression is then derived to approximately estimate the half-waves number m along x direction [32],

$$m^2 \cong \left(\frac{a}{b}\right)\left[\sqrt{\frac{k^2 D_{11} - 2k(D_{12}+2D_{66}) + D_{22}}{D_{11}}} - k\right] \tag{17}$$

For the case that m equals 1, the half-wave number n is given by,

$$n^2 \cong \frac{1}{k}\left(\frac{b}{a}\right)\left[\sqrt{\frac{D_{22} - 2k(D_{12}+2D_{66}) + k^2 D_{11}}{D_{22}}} - 1\right] \tag{18}$$

Eqs. (17) or (18) have limited applicability, because both contain two square root expressions. In a numerical procedure of searching roots m and n, Eqs. (17) and (18) are first verified. For instance, Eq. (17) is only used when both $\Delta_1 = (k^2 D_{11} - 2k(D_{12}+2D_{66}) + D_{22})/D_{11}$ and $\sqrt{\Delta_1} - k$ are positive, otherwise m is assigned to be 1. Eqs. (17) or (18) have limited applicability, because both contain two square root expressions. In a numerical procedure of searching m and n, Eqs. (17) and (18) are first verified. For instance, Eq. (17) is only used when both $\Delta_1 = (k^2 D_{11} - 2k(D_{12} + 2D_{66}) + D_{22})/D_{11}$ and $\sqrt{\Delta_1} - k$ are positive, otherwise m is assigned to be 1.

The end-shortening strains of a postbuckled rectangular laminated plate along x and y directions are calculated from [19],

$$\begin{aligned}\epsilon_x &= \frac{1}{ab}\int_0^a \int_0^b \left[a_{11}\frac{\partial^2 \Phi}{\partial y^2} + a_{12}\frac{\partial^2 \Phi}{\partial x^2} - \frac{1}{2}\left(\frac{\partial w}{\partial x}\right)^2\right]_{x=0,a} dxdy \\ &= (a_{11} + k a_{12})\left(\phi_x^{(0)} + \varepsilon^2 \phi_x^{(2)}\right) + \frac{1}{8}\varepsilon^2\left(\frac{m\pi}{a}\right)^2 + \frac{1}{4}\varepsilon^4 w_3 \left(\frac{m\pi}{a}\right)^2\end{aligned} \tag{19}$$

$$\begin{aligned}\epsilon_y &= \frac{1}{ab}\int_0^a\int_0^b\left[a_{12}\frac{\partial^2\Phi}{\partial y^2}+a_{22}\frac{\partial^2\Phi}{\partial x^2}-\frac{1}{2}\left(\frac{\partial w}{\partial y}\right)^2\right]_{y=0,b}dxdy \\ &= (a_{12}+ka_{22})\left(\phi_y^{(0)}+\varepsilon^2\phi_y^{(2)}\right)+\frac{1}{8}\varepsilon^2\left(\frac{n\pi}{b}\right)^2+\frac{1}{4}\varepsilon^4 w_3\left(\frac{n\pi}{b}\right)^2\end{aligned} \tag{20}$$

The maximum out-of-plane deflection of a plate in postbuckling regime is computed from a single half-wave,

$$w_{max} = \varepsilon w_1 + (w_3 - w_{13} - w_{31})\varepsilon^3 \tag{21}$$

Substituting the coefficients in Eqs. (10)-(13) into Eqs. (19)-(21), the end-shortening strain and maximum out-of-plane deflection function are written as,

$$\begin{aligned}\epsilon_x =&(a_{11}+ka_{12})N_x^{cr}+(N_{x0}-N_x^{cr})\left[(a_{11}+ka_{12})+\frac{2a_{11}a_{22}(1+k\alpha^2)}{a_{22}+a_{11}\alpha^4}\right]+ \\ &(N_{x0}-N_x^{cr})^2\frac{6b^2}{(n\pi)^2}\frac{(1+k\alpha^2)^2}{a_{22}^3+3a_{11}a_{22}^2\alpha^4+3a_{11}^2a_{22}\alpha^8+a_{11}^3\alpha^{12}}\cdot \\ &\left[\frac{a_{11}a_{22}^3(1+k\alpha^2)}{-8kD_{11}+16(D_{12}+2D_{66})+(80-72k\alpha^2)\alpha^2D_{22})}+\right. \\ &\left.\frac{a_{11}^3a_{22}\alpha^{10}(1+k\alpha^2)}{(72-80k\alpha^2)D_{11}+16k\alpha^4(D_{12}+2D_{66})-8\alpha^4D_{22}}\right]\end{aligned} \tag{22}$$

$$\begin{aligned}w_{max} =&\frac{4b}{n\pi}\left[\frac{(N_{x0}-N_x^{cr})(1+k\alpha^2)a_{11}a_{22}\alpha^2}{a_{22}+a_{11}\alpha^4}\right]^{\frac{1}{2}} \\ &\left\{1+\left(\frac{b}{n\pi}\right)^2\left[\frac{(N_{x0}-N_x^{cr})(1+k\alpha^2)^2a_{11}a_{22}\alpha^2}{2(a_{22}+a_{11}\alpha^4)^2}\right]\cdot\right. \\ &\left[\frac{(a_{22}-2a_{11}\alpha^4)/(a_{11}\alpha^2)}{-8kD_{11}+16(D_{12}+2D_{66})+(80-72k\alpha^2)\alpha^2D_{22}}\right. \\ &\left.\left.+\frac{\alpha^6(a_{11}\alpha^4-2a_{22})/a_{22}}{(72-80k\alpha^2)D_{11}+16k\alpha^4(D_{12}+2D_{66})-8\alpha^4D_{22}}\right]\right\}\end{aligned} \tag{23}$$

Note, the accuracy of the postbuckling model given by Eqs. (22) and (23) for biaxial compressive loaded plates with highly orthotropic material (E_1/E_2 is large) is not satisfactory, when the load ratio (k) and aspect ratio (a/b) are large. To accurately model such cases, more terms should be included in the perturbation expansion (7) and (8). However, to derive such a postbuckling model is cumbersome and out of the scope of this paper. From our numerical experience, Eqs. (22) and (23) is sufficiently accurate for highly orthotropic material when $k < 0.5$ and $a/b < 5$.

For the case that laminated plates are only subjected to a uniaxial compressive loading ($k =$

$0, N_{y0} = 0$), Eqs. (22) and (23) reduce to,

$$\begin{aligned}\epsilon_x =& a_{11}N_x^{cr} + (N_{x0} - N_x^{cr})(a_{11} + \frac{2a_{11}a_{22}}{a_{22} + a_{11}\alpha^4}) + \\ & \frac{6b^2}{(n\pi)^2}\frac{(N_{x0} - N_x^{cr})^2}{a_{22}^3 + 3a_{11}a_{22}^2\alpha^4 + 3a_{11}^2a_{22}\alpha^8 + a_{11}^3\alpha^{12}}. \\ & \left[\frac{a_{11}a_{22}^3}{16(D_{12} + 2D_{66}) + 80D_{22}\alpha^2} + \frac{a_{11}^3a_{22}\alpha^{10}}{72D_{11} - 8D_{22}\alpha^4}\right]\end{aligned} \tag{24}$$

$$\begin{aligned}w_{max} =& \frac{4b}{n\pi}\left[\frac{(N_{x0} - N_x^{cr})a_{11}a_{22}\alpha^2}{a_{22} + a_{11}\alpha^4}\right]^{\frac{1}{2}}\left\{1 + \left(\frac{b}{n\pi}\right)^2\left[\frac{(N_{x0} - N_x^{cr})a_{11}a_{22}\alpha^2}{2(a_{22} + a_{11}\alpha^4)^2}\right]\cdot\right. \\ & \left.\left[\frac{(a_{22} - 2a_{11}\alpha^4)/(a_{11}\alpha^2)}{16(D_{12} + 2D_{66}) + 80\alpha^2D_{22}} + \frac{\alpha^6(a_{11}\alpha^4 - 2a_{22})/a_{22}}{72D_{11} - 8\alpha^4D_{22}}\right]\right\}\end{aligned} \tag{25}$$

As such, in Eqs. (22) and (23), the end-shortening strain (ϵ_x) and maximum transverse deflection (w_{max}) of a postbuckled rectangular plate are expressed as nonlinear functions of applied external (compression) load. The nonlinearity of the postbuckling equilibrium path is explicitly defined in terms of the composite stiffnesses (a_{ij}, D_{ij}), plate aspect ratio (k) and external loading ($N_{x0} - N_x^{cr}$). If the nonlinear terms (with respect to the applied compression loading) are ignored and only the linear terms are retained, Eq. (22) reduces to the same form as Harris's model [22].

III. Lamination parameters

In the determination of Eqs. (22) and (23), the in-plane and bending stiffness of an orthotropic laminated plate are expressed in terms of four lamination parameters as,

$$\begin{bmatrix} A_{11} \\ A_{12} \\ A_{22} \\ A_{66} \end{bmatrix} = h \begin{bmatrix} 1 & \xi_1^A & \xi_2^A & 0 & 0 \\ 0 & 0 & -\xi_2^A & 1 & 0 \\ 1 & -\xi_1^A & \xi_2^A & 0 & 0 \\ 0 & 0 & -\xi_2^A & 0 & 1 \end{bmatrix} \begin{bmatrix} U_1 \\ U_2 \\ U_3 \\ U_4 \\ U_5 \end{bmatrix} \tag{26}$$

$$\begin{bmatrix} D_{11} \\ D_{12} \\ D_{22} \\ D_{66} \end{bmatrix} = \frac{h^3}{12} \begin{bmatrix} 1 & \xi_1^D & \xi_2^D & 0 & 0 \\ 0 & 0 & -\xi_2^D & 1 & 0 \\ 1 & -\xi_1^D & \xi_2^D & 0 & 0 \\ 0 & 0 & -\xi_2^D & 0 & 1 \end{bmatrix} \begin{bmatrix} U_1 \\ U_2 \\ U_3 \\ U_4 \\ U_5 \end{bmatrix} \tag{27}$$

where U_1, U_2, U_3, U_4, U_5 are material invariants of composite [33]. The in-plane compliance constants a_{ij} in terms of lamination parameters are obtained from the in-plane stiffness A_{ij} by the expressions,

$$a_{11} = \frac{A_{22}}{A_{11}A_{22} - A_{12}^2}, \quad a_{12} = -\frac{A_{12}}{A_{11}A_{22} - A_{12}^2}$$
$$a_{22} = \frac{A_{11}}{A_{11}A_{22} - A_{12}^2}, \quad a_{66} = \frac{1}{A_{66}} \tag{28}$$

$\xi_{1,2}^A$ and $\xi_{1,2}^D$ are the in-plane and out-of-plane lamination parameters respectively and defined as,

$$\xi_{[1,2]}^A = \frac{1}{2}\int_{-1}^{1} [\cos(2\theta(\bar{z}))\cos(4\theta(\bar{z}))] d\bar{z} \tag{29}$$

$$\xi_{[1,2]}^D = \frac{3}{2}\int_{-1}^{1} [\cos(2\theta(\bar{z}))\cos(4\theta(\bar{z}))] \bar{z}^2 d\bar{z} \tag{30}$$

where $\theta(\bar{z})$ is the layup function in the thickness direction of the plate.

Optimal laminates are determined using lamination parameters as design variables. The benefit of using lamination parameters over ply angles is that the entire design space is represented, regardless of the number of plies, by a fixed number of variables. The optimal lamination parameters for a given application, therefore, represent the optimal design for particular lamina type rather than a stacking sequence. Once they are known the task becomes the computation of the laminate which most closely meets the optimal lamination parameters. In the current work, a two-level optimization procedure was carried out to determine the layups given the optimal postbuckling behaviour [26]. The two-level approach has been applied as an effective means [25] to solve complex optimization problems that are involved in the design of composite laminates. Recently, it was successfully applied to solve a challenge optimization problem for tow-steering composite laminates [35], which possess spatially varying material properties.

Previous optimization works [26] employed an outer boundary of the feasible region of lamination parameters. In plate postbuckling, a strong coupling between the in-plane stiffness and out-of-plane stiffness is present. Consequently, an accurate boundary of the feasible region of lamination parameters is important for obtaining meaningful optimal solutions. Based on the work in Wu *et al.* [34, 35], such a boundary for $\xi_{1,2}^A$ and $\xi_{1,2}^D$ is defined by the following equations.

$$5(\xi_1^A - \xi_1^D)^2 - 2(1 + \xi_2^A - 2(\xi_1^A)^2) \leq 0 \tag{31}$$

$$(\xi_2^A - 4t\xi_1^A + 1 + 2t^2)^3 - 4(1 + 2|t| + t^2)^2(\xi_2^D - 4t\xi_1^D + 1 + 2t^2) \leq 0 \tag{32}$$

$$(4t\xi_1^A - \xi_2^A + 1 + 4|t|)^3 - 4(1 + 2|t| + t^2)^2(4t\xi_1^D - \xi_2^D + 1 + 4|t|) \leq 0 \tag{33}$$

where $t = [-1, -0.75, -0.5, -0.25, 0, 0.25, 0.5, 0.75, 1]$(or, for better accuracy, $t = [-1, -0.8, -0.6, -0.4, -0.2, 0, 0.2, 0.4, 0.6, 0.8, 1]$). It has been shown that these $19 \sim 23$ equations in (31)-(33) are able to bound the feasible region of the four lamination parameters ($\xi_{1,2}^{A,D}$).

IV. Optimum Laminate Design

A. Optimization criteria

In the design of compression-loaded plates, the objective is to compute the lightest structure subject to constraints of stiffness, strength and stability. Traditionally, this process is performed on the basis of a linear extrapolation of the plate behaviour made about the stress-free state. In the present work we augment this process in two ways. Firstly, we remove the constraint on the buckling load. The structure is free to buckle as long as it can continue to take further loading. Secondly, the stiffness constraints are imposed on the structure at any point along the equilibrium path. In the optimization problem the objectives are to minimize either the end-shortening strain ϵ_x ($=\Delta_x/a$) along the loading direction or the maximum transverse deflection w_{max} under a prescribed service load N_{x0}. As the applied loading condition is identical for each optimal design, the overall structural strength, or the load-carrying capacity, directly relates to the resultant end-shortening strain or the maximum transverse deflection. Their evaluation is based on the postbuckling equilibrium paths, which are the nonlinear load-transverse deflection and the load-end shortening curves.

The load and strain in the postbuckling equilibrium paths are normalised with respect to the corresponding solutions of the quasi-isotropic plate. This normalisation provides the designer with a

useful measure to quantify the improvement of an optimal laminate over the quasi-isotropic laminate [26]. The equivalent Young's modulus E_{iso}, Poisson's ratio ν_{iso} and bending stiffness D_{iso} of the quasi-isotropic laminate are given by [26, 36],

$$D_{iso} = \frac{E_{iso}h^3}{12(1-\nu_{iso}^2)}, \quad \nu_{iso} = \frac{U_4}{U_1}, \quad E_{iso} = U_1(1-\nu_{iso}^2) \tag{34}$$

B. First-level optimal design

In the postbuckling response of constant stiffness laminated plates, the optimization problem is stated as follows:

Minimize:

$$\epsilon_x(\boldsymbol{\xi})/\epsilon_x^{iso} \quad \text{or} \quad w_{max}(\boldsymbol{\xi})/h \tag{35}$$

Design Variables:

$$\boldsymbol{\xi} = \left[\xi_1^A,\ \xi_2^A,\ \xi_1^D,\ \xi_2^D\right] \tag{36}$$

subject to:

$$g_j(\boldsymbol{\xi}) \leqslant 0 \tag{37}$$

where g_j are the constraint functions in Eqs. (31)-(33) that define the feasible region of these four lamination parameters.

In a GCMMA approach [37], the objective function and the nonlinear constraints are approximated by convex separable forms in a local region as [37],

$$\bar{f}_i^{(\mu,\nu)}(\boldsymbol{\xi}) = \sum_{j=1}^{4}\left(\frac{p_{ij}^{(\mu,\nu)}}{\alpha_j^{(\mu)} - \xi_j} + \frac{q_{ij}^{(\mu,\nu)}}{\xi_j - \beta_j^{(\mu)}}\right) + r_i^{(\mu,\nu)} \tag{38}$$

where μ and ν denote the indices of the "outer" and "inner" iterations, respectively. For the detailed expression of each variable in Eq. (38) refer to Svanberg's work[37]. The approximating formula of Eq. (38) for the objective function and nonlinear constraints is shown to be convex separable and conservative with respect to the each design variable (lamination parameters). The advantages of applying the GCMMA approach is that the feasible constraints can be strictly satisfied in an optimization process and there is a strong likelihood of finding the globally optimal solution.

C. Second-level optimal design

The objective of the second level optimization process is to retrieve a realistic layup. An anti-symmetrical stacking sequence with specially orthotropic properties ($[B] = 0$, $A_{16}, A_{26} = 0$, $D_{16}, D_{26} = 0$) is used. For instance, the stacking sequence with a 16-layer laminate $[\pm\theta_1/\mp\theta_1/\pm\theta_2/\mp\theta_2]_{AS}$ possesses two independent ply varying-orientations. Larger design freedoms can be achieved in the second level optimization process by adding more design layers. Subsequently, a GA is used to determine the fibre orientation angles for each design layer which results in lamination parameters matching the desired results closely. The fitness function is expressed as a mean value of the least square distance between the obtained lamination parameters and the target lamination parameters evaluated at a large number of points ($2000 \sim 5000$) in the plate[26]. The optimization problem is formulated as,

$$\begin{aligned} \textbf{min} \quad & \Delta\xi(\theta_i) = \left[\sum_i^2 w_i^A \left(\xi_i^A - \tilde{\xi}_i^A\right)^2 + \sum_i^2 w_i^D \left(\xi_i^D - \tilde{\xi}_i^D\right)^2\right] \\ & \xi_{1,2}^{A,D} \leftarrow [\theta_1, \theta_2, \theta_3, \theta_4] \\ \textbf{s.t.:} \quad & -\pi/2 \leqslant \theta_i \leqslant \pi/2 \end{aligned} \tag{39}$$

where θ_i is the fibre angle at each design layer and w_i^A and w_i^D are the weights to distinguish the relative importance between $\xi_{1,2}^A$ and $\xi_{1,2}^D$. Based on our trial-and-error experiences, the population size was set to be at least $20 \sim 30$ times the number of design variables, while the number of generations is usually set to $50 \sim 100$ depending on the population size. The crossover and mutation probabilities were chosen to be 0.7 and 0.04

V. Results and Discussion

In this section, rectangular laminated plates subjected to a uniform axial displacement compression are optimized in their postbuckling regime. The composite lamina properties of MTM49-3/T800 are given by $E_1 = 163$GPa, $E_2 = 6.8$GPa, $G_{12} = 3.4$GPa, $\nu_{12}= 0.28$. The plate thickness is 4.2 mm (for 32 layers). The plate width (b) is 0.5 m and the aspect ratio (a/b) is 1, 2 or 5 for different case study.

A. Model validation

Numerical results for the postbuckling behaviour of a laminated plate under uniaxial compression given by Eqs. (24) and (25) are compared with the numerical results given by finite-element method (FEM) and other postbuckling models. The FEM postbuckling analyses of composite plates were carried out using commercial code ABAQUS. The S4 shell element was chosen for discretization of the plate structure and a sufficient mesh density was selected to achieve convergence. In addition, the nodes along each edge are constrained to satisfy the in-plane boundary conditions defined by Eq. (6). Numerical results for the postbuckling behaviour of a laminated plate under uniaxial compression given by Eqs. (24) and (25) are compared with the numerical results given by finite-element method (FEM) and other postbuckling models. The FEM postbuckling analyses of composite plates were carried out using commercial code ABAQUS. A small imperfection in the form of the first buckling mode shape and a magnitude of 1% of the plate thickness is included in each finite element models.

A unidirectional laminate $[0]_s$ is chosen for the postbuckling model validation. It was found that perturbation methods yield the least accurate solutions for the $[0]_s$ laminates with the material properties that are highly orthotropic (the ratio of E_1/E_2 is large). Figure 2 illustrates the postbuckling equilibrium paths of a $[0]_s$ plate given by various analytical models and the FEM. Figure 2-a gives the normalised strains $\epsilon_x/\epsilon_x^{iso}$ as a function of the normalised axial loads N_{x0}/N_x^{iso}. Figure 2-b shows the normalised maximum transverse displacement w_{max}/h as a function of the normalised axial loads N_{x0}/N_x^{iso}. It can be seen that the present method gives a relatively accurate solution, whereas Zhang and Shen's model fails to capture the structural behaviour in the deep postbuckling regime. It also approves Eqs. (22) and (23) or (24) and (25) that can accurately predict moderately deep postbuckling behaviour of highly orthotropic composite plates. Harris's model is only valid for predicting the initial postbuckling response. As the results shown in Figure 2 are an extreme case, the present closed-form solutions given by Eqs. (22) and (23) are sufficiently accurate for performing the postbuckling optimization.

From our numerical experience on some extreme cases, our postbuckling solution remains valid when the postbuckling equilibrium path has achieved a point where $w/h = 1.5 \sim 2$. Hence, quan-

titatively speaking, the "moderately deep postbuckling" in this paper refers to the out-of-plane deflection of a postbuckled plate where w is $1.5 \sim 2$ times of the plate thickness h.

B. Optimal results

1. Optimal lamination parameters (first-level)

Two types of problems were studied for the postbuckling optimization: (i) laminated plates under uniaxial compression with different aspect ratios ($a/b = 1, 2, 5$), and (ii) square laminated plates under biaxial compression with different loading ratios ($k = 0.1, 0.2, 0.5$). The lamination parameters obtained from the first-level optimization procedures are demonstrated in Tables 1-4. Tables 1 and 3 give the optimum laminates for minimizing end-shortening strain, whereas Tables 2 and 4 show the optimum designs for minimizing the maximum transverse deflection.

The optimal laminate configuration which gives minimum end-shortening strain or maximum transverse displacement may be different when the level of axial load (N_{x0}) is changed. The postbuckling optimization for each case is carried out with respect to several axial loads. As shown in Tables 1-4, the value of axial load N_{x0} is varied from $1.5N_x^{iso}$, $2N_x^{iso}$ and $2.5N_x^{iso}$ for both minimising the end-shortening strain and the maximum transverse displacement.

As shown in Table 1, for the square laminated plate ($a/b = 1$) under uniaxial compression, the optimal lamination parameters that give the minimum end-shortening strain are different with respect to different axial compressive load (N_{x0}). For the case where the length of a plate is twice its width ($a/b = 2$), the optimal lamination parameters are similarly valued for different values of N_{x0}. When the aspect ratio increases to 5 (a long plate), the optimal lamination parameters are nearly identical irrespective of the level of axial loading. Minimising the maximum transverse deflection, as shown in Table 2, the optimal lamination parameters are different for different given axial loading (N_{x0}). However, for a fixed level of axial loading, the optimal lamination parameters remain similar when the aspect ratio of plate is changed. This is due to the fact that the buckling/postbuckling mode shapes of simply supported orthotropic plates are periodic sine waves and the maximum transverse deflection only depends on the amplitude of a half-wave.

For the cases of biaxial compressive loading, the postbuckling behaviour of square laminated

plates with three different loading ratios ($k = 0.1, 0.2, 0.5$) was optimized. As shown in Table 3, the optimal lamination parameters that give the minimum end-shortening strain are different with respect to different axial compressive load (N_{x0}). It was also noticed that the optimal lamination parameters for the cases where $k = 0.1$ and $k = 0.2$ are close in value to each other, whereas the optimal lamination parameters for the loading ratio $k = 0.5$ are quite different. This behaviour reflects the structural behaviour of the postbuckled plates is mainly dominated by the longitudinal compressive loading when k is small. With the increase of loading ratio k, the structural behaviour is more affected by the transverse compressive loading and thus it results in different optimal laminate configuration. The optimal lamination parameters that minimized the maximum transverse deflection of biaxially loaded plates, as shown in Table 4, match well for different loading ratios (k). Unlike the results shown in Table 2, changing the loading condition (the value of k) results in slightly different optimal solutions. It was also found that, the aspect ratio also has little effect on the optimal results for minimising the maximum transverse deflection of a biaxially loaded plate.

2. Optimal layups (second-level)

We now discuss the optimal layups obtained from second-level optimization procedure for the uniaxial compression loaded plates. It was found that many lamination configurations exist that closely match the target lamination parameters. The layups presented in Tables 5 and 6 provide the solutions that are given by the specially orthotropic stacking sequence. In most cases, 4 or 5 design layers (32 or 40 plies) were used in the optimization process for achieving desired accuracy. The values in last columns of Tables 5 and 6 denote the difference of optimal buckling load between second level optimization and first level in terms of lamination parameters. It can be seen that the postbuckling behaviour given by the optimal layups matches well with that given by the optimal lamination parameters. For a square plate, the layup $[\pm 45/\mp 45/0_{12}]_{AS}$ gives the minimum end-shortening strain (ϵ_x). The normalised end-shortening strain for a fixed axial load gives a direct measure of the effective structural stiffness, is a function of the normalised quantities of prebuckling stiffness ($\bar{K}_{pre}$), buckling load ($\bar{N}_x^{cr}$) and postbuckling stiffness ($\bar{K}_{post}$) given by,

$$\frac{\epsilon_x}{\epsilon_x^{iso}} = \frac{\bar{N}_x^{cr}}{\bar{K}_{pre}} + \frac{\bar{N}_{x0} - \bar{N}_x^{cr}}{\bar{K}_{post}} = \frac{\bar{N}_{x0}}{\bar{K}_{post}} - (\frac{1}{\bar{K}_{post}} - \frac{1}{\bar{K}_{pre}})\bar{N}_x^{cr} \tag{40}$$

From this expression (for $\bar{K}_{post} < \bar{K}_{pre}$) and for a given value of $\bar{N}_{x0}$ then end-shortening strain reduces for increasing values of $\bar{K}_{post}$, $\bar{K}_{pre}$ and $\bar{N}_x^{cr}$. To minimize the end-shortening strain of a compression-loaded laminate, a large proportion of 0-deg plies in the laminate is important for carrying the compression load and also for improvement of pre- and postbuckling stiffness of the plate. In addition, the presence of ±45-deg plies in the outer layers improves the critical buckling load of the laminate. As such, the $[\pm 45/\mp 45/0_{12}]_{AS}$ layup gives the minimum end-shortening strain to the square laminates.

In the case of rectangular plates ($a/b = 2$ and 5), the 0-deg plies for a laminate are found to be preferential for a high pre-buckling stiffness, while the outer ply angles for the optimal stacking sequences are slightly different (65 and 70, respectively) from those of the square plate. The optimal laminates for postbuckling having the minimum w_{max} with respect to different values of axial load N_{x0} are shown in Table 2. It is observed that in this optimization problem a large number of 90-deg plies were dominant. Their role is to suppress the out-of-plane deflection in the post-buckling regime by providing a high bending stiffness in the y-direction.

The postbuckling equilibrium paths of the optimized laminates (for square plates) are compared and illustrated in Figures 3 and 4. The FEM results are also illustrated to validate the postbuckling analysis given by the closed-form solutions. It is shown that the closed-form model accurately predicts the postbuckling response of laminated plates. In Figure 3, the postbuckling behaviour of the layups $[\pm 45/\mp 45/0_{12}]$ and $[\pm 65/\mp 65/0_{12}]$ match well because both of the layups possess a large proportion of 0-deg piles. These two laminates give slightly improved buckling load but much higher pre- and postbuckling stiffness comparing with the quasi-isotropic laminate. In Figure 4, the optimal layups $[\pm 60/\mp 60/\pm 75/\mp 75/90_4/0_8]_{AS}$ and $[\pm 68/\mp 68/90_8/0_8]_{AS}$ demonstrate significant improvement for minimising the maximum transverse deflection (over 30%). However, their axial stiffnesses in the pre- and postbuckling regime are slightly poorer than that of quasi-isotropic laminate, as shown in Figure 4.

For the biaxial compressive loading conditions ($k = 0.2$), laminate layups were retrieved and their postbuckling behaviour are demonstrated in Figs. 5 and 6. As shown in Fig. 5, the layup $[\pm 35/\mp 35/\pm 20/\mp 20/0_8]_{AS}$ gives the minimum end-shortening strain for the axial loading $N_{x0} =$

$1.5N_x^{iso}$ and $[\pm 50/\mp 50/\pm 10/\mp 10/0_8]_{AS}$ is the optimized layup for the minimum end-shortening strain when axial loading $N_{x0} = 2N_x^{iso}$ or $N_{x0} = 2.5N_x^{iso}$. It shows that a large proportion of 0-deg plies in a laminate is also important for minimising the end-shortening strains for biaxial compressive loading cases. In Fig. 6, the layup $[(\pm 45/\mp 45)_2/\pm 75/\mp 75/0_4]_{AS}$ shows the minimum of maximum transverse deflection when $N_{x0} = 1.5N_x^{iso}$, whereas $[\pm 60/\mp 60/\pm 90/\mp 90/0_8]_{AS}$ and $[\pm 70/\mp 70/\pm 90/\mp 90/0_8]_{AS}$ are the optimized layups for $N_{x0} = 2N_x^{iso}$ and $N_{x0} = 2.5N_x^{iso}$, respectively. Compared with the optimal layups in Figs. 4 and 6, we observe that the inner layers of all of these layups are always a combination of $[90_n/0_n]$, which is beneficial for a laminate to minimize its membrane strains and hence its nonlinear, in the von Kármán's sense, maximum transverse deflection.

VI. Conclusion

An enhanced perturbation model for the moderately deep postbuckling analysis of rectangular composite plates under biaxial compression loading has been presented. The end-shortening strain and the maximum deflection of composite plates in the postbuckling regime are expressed in closed-form as a function of the applied axial loads. The newly derived closed-form expressions (Eqs. 24 and 25) not only provide a straightforward means to predict the postbuckling response of orthotropic composite laminates but also facilitate rapid conceptual design. The postbuckling solutions have been validated against FEM results and were shown to be sufficiently accurate for use in an optimization routine. The closed-form expressions and the two-level optimization method can be readily implemented as a tool in practical composite structural design.

A two-level optimization strategy was carried out for the optimal design of the postbuckling behaviour of laminated composite plates. The optimal laminate layups were determined for either minimizing the end-shortening strain or minimizing the maximum transverse deflection. Numerical examples are studied on the laminated plate with different aspect ratios and with different loading ratios. From the optimization results, it was observed, in general, that a layup with a large proportion of 0-deg piles possesses high compressive postbuckling resistance, while a combination of $[90_n/0_n]$ for the inner layers of a layup is beneficial suppressing the transverse deflection in the

postbuckling regime.

Table 1 Optimal design for minimizing the end-shortening strain ϵ_x of plates under uniaxial compression

Plate	Loads	Lamination parameters				$\epsilon_x/\epsilon_x^{iso}$
	(N_{x0}/N_x^{iso})	ξ_1^A	ξ_2^A	ξ_1^D	ξ_2^D	
	1.5	0.74	0.53	0.42	-0.10	1.11
$a/b=1$	2.0	0.70	0.72	0.30	0.28	1.82
	2.5	0.67	0.79	0.19	0.45	2.52
	1.5	0.62	0.795	0.845	0.476	0.90
$a/b=2$	2.0	0.63	0.778	0.83	0.40	1.27
	2.5	0.62	0.79	0.839	0.445	1.66
	1.5	0.71	0.999	0.99	0.996	0.85
$a/b=5$	2.0	0.69	1.00	0.99	1.00	1.19
	2.5	0.68	1.00	0.99	1.00	1.55

Table 2 Optimum design for minimizing maximum transverse displacement w_{max} of plates under uniaxial compression

Plate	Loads	Lamination parameters				w_{max}/h
	(N_{x0}/N_x^{iso})	ξ_1^A	ξ_2^A	ξ_1^D	ξ_2^D	
	1.5	0.018	-0.016	-0.20	-0.76	0.86
$a/b=1$	2.0	-0.144	0.61	-0.61	0.05	1.29
	2.5	-0.245	0.833	-0.787	0.54	1.53
	1.5	0.018	-0.016	-0.20	-0.76	0.86
$a/b=2$	2.0	-0.144	0.61	-0.61	0.05	1.29
	2.5	-0.245	0.833	-0.787	0.54	1.53
	1.5	0.018	-0.016	-0.20	-0.76	0.86
$a/b=5$	2.0	-0.144	0.61	-0.61	0.05	1.29
	2.5	-0.245	0.833	-0.787	0.54	1.53

Acknowledgments

The authors wish to acknowledge EPSRC, Airbus and GKN for supporting this research under the project ABBSTRACT2 (EP/H026371/1).

[1] S. B. Dickson, J. N.; Biggers, Postop: Postbuckled open-stiffener optimum panels - theory and capability, NASA/CR-172259 (January, 1984) 1–39.

[2] D. Shin, Z. Gürdal, and O.H. Griffin, Jr, Minimum weight design of laminated composite plates postbuckling performance, Applied Mechanics Reviews 44 (11) (1991) 219 – 231

[3] D. Bushnell, Optimization of composite, stiffened, imperfect panels under combined loads for service in the postbuckling regime, Computer Methods in Applied Mechanics and Engineering 103 (1-2) (1993) 43 – 114.

[4] S. Adali, M. Walker, V.E. Verijenko, Multiobjective optimization of laminated plates for maximum prebuckling, buckling and postbuckling strength using continuous and discrete ply angles, Composite Structures 35 (1) (1996) 117 âĂŞ- 130.

[5] C. A. Perry, Z. Gürdal, J. H. Starnes, Minimum-weight design of compressively loaded stiffened panels for postbuckling response, Engineering Optimization 28 (3) (1997) 175–197.

[6] O. Seresta, M. Abdalla, Z. Gürdal, Optimal Design of Laminated Composite Plate for Maximum Postbuckling Strength, 46th AIAA/ASME/ASCE/AHS/ASC Structures, Structural Dynamics and Materials Conference Austin, Texas

[7] Ji-Ho Kang, Chun-Gon Kim, Minimum-weight design of compressively loaded composite plates and stiffened panels for postbuckling strength by Genetic Algorithm, Composite Structures 69 (2) (2005) 239 – 246.

[8] R. Rikardsa, H. Abramovichb, K. Kalninsa, J. Auzinsa, Surrogate modelling in design optimization of stiffened composite shells, Composite Structures 73 (2) (2006) 244 -âĂŞ 251.

[9] L. Lanzi, V. Giavotto, Post-buckling optimization of composite stiffened panels: Computations and experiments, Composite Structures 73 (2006) 208 âĂŞ- 220.

[10] O. Bacarreza, M. H. Aliabadi, A. Apicella, Robust design and optimization of composite stiffened panels in post-buckling, Structural and Multidisciplinary Optimization 51 (2) (2015) 409 – 422.

[11] E. Barkanova, E. Eglitisa, F. Almeidab, M.C. Boweringb, G. Watsonb, Optimal design of composite lateral wing upper covers. Part II: Nonlinear buckling analysis, Aerospace Science and Technology 51 (2016) 87 âĂŞ- 95.

[12] S. Henrichsen, P. Weaver, E. Lindgaard, E. Lund, Post-buckling optimization of composite structures using Koiter's method, International Journal for Numerical Methods in Engineering (2016).

[13] Y. Mo, D. Ge, B. He, Experiment and optimization of the hat-stringer-stiffened composite panels under axial compression, Composites Part B 84 (2016) 285 – 293.

[14] F. Stoll, Z. Gürdal, J. H. Starnes, A method for the geometrically nonlinear analysis of compressively loaded prismatic composite structures, NASA/CR 2002- 211919 (February 1991) 1–14.

[15] M. Lillico, R. Butler, G. Hunt, A. Watson, D. Kennedy, F. Williams, Analysis and testing of a post-buckled stiffened panel, AIAA Journal 40 (5) (2002) 996 – 1000.

[16] W. Liu, R. Butler, A. R. Mileham, A. J. Green, Bilevel optimization and postbuckling of highly strained composite stiffened panels, AIAA Journal 44 (11) (2006) 2562–2570.

[17] K. Marguerre, The apparent width of the plate in compression, NACA, Report No. 833.

[18] S. Levy, Bending of rectangular plates with large deflections, NACA, Report No. 737.

[19] J. M. Coan, Large deflection theory for plates with small initial curvature loaded in edge compression, Journal of Applied Mechanics 18 (1950) 143–151.

[20] N. Yamaki, Postbuckling behavior of rectangular plates with small initial curvature loaded in edge compression, Journal of Applied Mechanics 26 (1959) 407Öf14.

[21] M. Stein, Loads and deformations of buckled rectangular plates, NASA Tech. Rep. R-40.

[22] G. Harris, The buckling and post-buckling behaviour of composite plates under biaxial loading, International Journal of Mechanical Sciences 17 (3) (1975) 187 – 202.

[23] R. Chandra, B. Raju, Postbuckling analysis of rectangular orthotropic plates, International Journal of Mechanical Sciences 15 (1) (1973) 81 – 97.

[24] J. Zhang, H. Shen, Postbuckling of orthotropic rectangular plates in biaxial compression, Journal of Engineering Mechanics 117 (5) (1991) 1158–1170.

[25] K. Yamazaki, Two-level optimization technique of composite laminate panels by genetic algorithms, Collection of Technical Papers - AIAA/ASME/ASCE/AHS/ASC Structures, Structural Dynamics and Materials Conference 3 (1996) 1882 – 1887.

[26] C. G. Diaconu, P. M. Weaver, Approximate solution and optimum design of compression-loaded, post-buckled laminated composite plates, AIAA Journal 43 (4) (2005) 906 – 914.

[27] E. H. Mansfield, The bending and stretching of plates, Second Edition, Cambridge University Press, 1989.

[28] P. S. Bulson, The Stability of Flat Plates, Chatto and Windus Ltd, London, 1970.

[29] Z. Wu, G. Raju, P. M. Weaver, Postbuckling analysis of variable angle tow composite plates, International Journal of Solids and Structures 60 (0) (2013) 163 – 172.

[30] H. Shen, J. Zhang, Perturbation analyses for the postbuckling of simply supported rectangular plates

under uniaxial compression, Applied Mathematics and Mechanics 9 (1988) 793–804.

[31] C. Libove, Buckle pattern of biaxially compressed simply supported orthotropic rectangular plates., Journal of Composite Materials 17 (1) (1983) 45 – 48.

[32] T. Tung, J. Surdenas, Buckling of rectangular orthotropic plates under biaxial loading., Journal of Composite Materials 21 (2) (1987) 124 – 128.

[33] R. M. Jones, Mechanics of composite materials, CRC Press, 2nd Revised edition edition, 1998.

[34] Z. Wu, G. Raju, P. M. Weaver, Feasible region of lamination parameters for optimization of variable angle tow (vat) composite plates, Collection of Technical Papers - 54rd AIAA/ASME Structures, Structural Dynamics and Materials Conference.

[35] Z. Wu, G. Raju, P. M. Weaver, Framework for the buckling optimization of variable-angle tow composite plates, AIAA Journal 53 (12) (2015) 3788 – 3804.

[36] M. Pandey, A. Sherbourne, Postbuckling behaviour of optimized rectangular composite laminates, Composite Structures 23 (1) (1993) 27 – 38.

[37] K. Svanberg, Mma and gcmma, versions september 2007.

[38] B. Budiansky, Theory of Buckling and Post-Buckling Behavior of Elastic Structures, Advances in Applied Mechanics Volume 14 (1974) 1 -âĂŞ 65

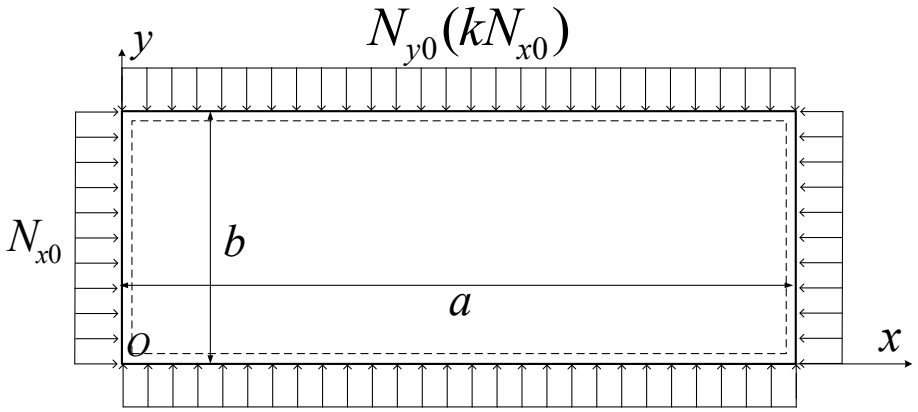

Fig. 1 Load, geometry and boundary conditions of plates

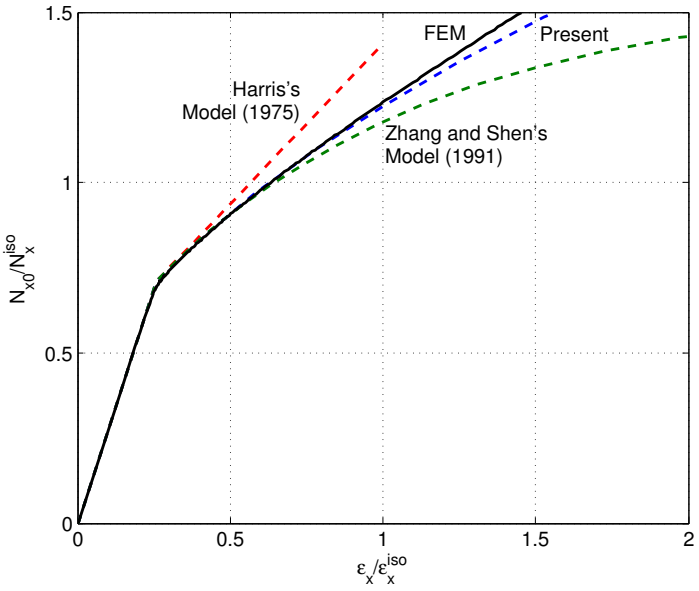

(a)

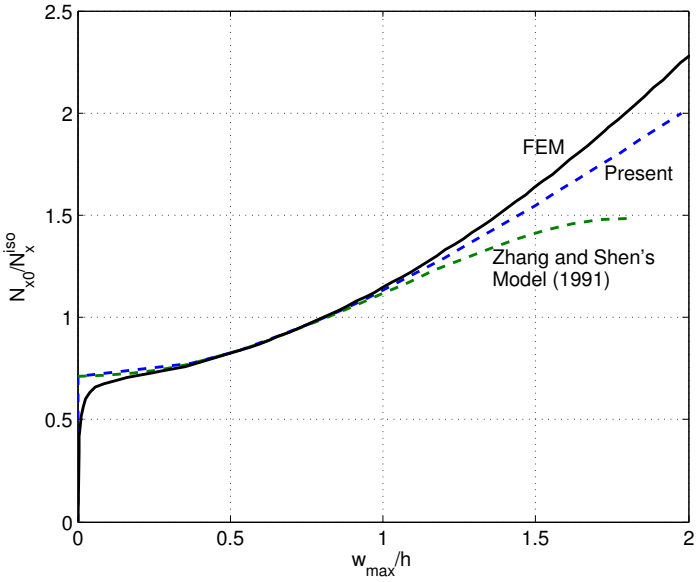

(b)

Fig. 2 Postbuckling model validation and comparison: (a) Normalised axial loads N_x/N_x^{iso} versus Normalised axial strain $\epsilon_x/\epsilon_x^{iso}$ of for a $[0]_s$ laminate (b) Normalised axial loads N_x/N_x^{iso} versus Normalized maximum transverse displacement w_{max}/h function for a $[0]_s$ laminate.

Table 3 Optimal design for minimizing the end-shortening strain ϵ_x of a square plate $(a/b = 1)$ under biaxial compression $(k = N_{y0}/N_{x0})$

Plate	Loads	Lamination parameters				$\epsilon_x/\epsilon_x^{iso}$
	(N_{x0}/N_x^{iso})	ξ_1^A	ξ_2^A	ξ_1^D	ξ_2^D	
	1.5	0.77	0.45	0.45	-0.23	1.14
$k = 0.1$	2.0	0.68	0.60	0.30	0.038	1.97
	2.5	0.64	0.78	0.15	0.42	2.77
	1.5	0.77	0.33	0.54	-0.41	1.14
$k = 0.2$	2.0	0.69	0.49	0.30	-0.16	2.11
	2.5	0.60	0.70	0.12	0.23	3.05
	1.5	0.68	0.11	0.41	-0.66	1.07
$k = 0.5$	2.0	0.65	0.24	0.26	-0.52	2.58
	2.5	0.53	0.45	0.07	-0.23	4.1

Table 4 Optimum design for minimizing maximum transverse displacement w_{max} of a square plate $(a/b = 1)$ under biaxial compression $(k = N_{y0}/N_{x0})$

Plate	Loads	Lamination parameters				w_{max}/h
	(N_{x0}/N_x^{iso})	ξ_1^A	ξ_2^A	ξ_1^D	ξ_2^D	
	1.5	0	-0.11	-0.126	-0.82	0.91
$k = 0.1$	2.0	0.02	0.55	-0.49	-0.07	1.39
	2.5	-0.05	0.75	-0.64	0.35	1.67
	1.5	0.00	-0.106	-0.12	-0.82	0.90
$k = 0.2$	2.0	-0.06	0.64	-0.58	0.097	1.38
	2.5	-0.12	0.85	-0.74	0.57	1.64
	1.5	0.02	-0.12	-0.155	-0.83	0.90
$k = 0.5$	2.0	-0.04	0.58	-0.56	0.03	1.32
	2.5	-0.01	0.63	-0.55	0.08	1.49

Table 5 Optimal laminate layups for minimizing normalised end-shortening strain $\epsilon_x/\epsilon_x^{iso}$ of rectangular plates with different aspect ratios under uniaxial compression

Plate & Mode	N_{x0}/N_x^{iso}	Laminate configuration	$\epsilon_x/\epsilon_x^{iso}$	Difference
$a/b=1$	1.5	$[\pm 45/\mp 45/0_{12}]_{AS}$	1.11	0%
(m,n)=(1,1)	2	$[\pm 65/\mp 65/0_{12}]_{AS}$	1.83	0
	2.5	$[\pm 70/\mp 70//0_{12}]_{AS}$	2.52	0%
$a/b=2$	1.5	$[\pm 23/\mp 23/0_{12}/90_4]_{AS}$	0.92	2.17%
(m,n)=(2,1)	2	$[\pm 25/\mp 25/0_{12}/90_4]_{AS}$	1.33	5.2%
	2.5	$[\pm 25/\mp 25/0_{12}/90_4]_{AS}$	1.73	4%
$a/b=5$	1.5	$[0_{20}/90_4]_s$	0.87	2.3%
(m,n)=(5,1)	2	$[0_{20}/90_4]_s$	1.21	1.6
	2.5	$[0_{20}/90_4]_s$	1.56	0.6%

Table 6 Optimal laminate layups for minimizing the maximum transverse deflection w_{max}/h of rectangular plates with different aspect ratios under uniaxial compression

Plate & Mode	N_{x0}/N_x^{iso}	Laminate configuration	$\epsilon_x/\epsilon_x^{iso}$	Difference
$a/b=1,2,5$	1.5	$[(\pm 50/\mp 50)_2/\pm 25/\mp 25/90_4/0_4]_{AS}$	0.91	5%
(m,n)=(a/b,1)	2	$[\pm 60/\mp 60/\pm 75/\mp 75/90_4/0_8]_{AS}$	1.31	1.5%
	2.5	$[\pm 68/\mp 68/90_8/0_8]_{AS}$	1.54	1%

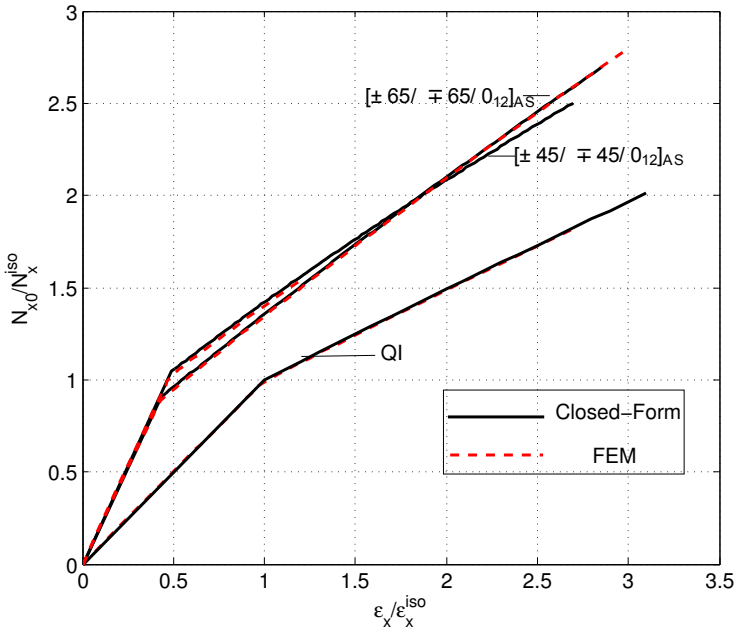

Fig. 3 Postbuckling responses of the optimal layups of a square plate under uniaxial compression for minimizing the end-shortening strain: Normalised axial loads N_x/N_x^{iso} versus Normalised axial strain $\epsilon_x/\epsilon_x^{iso}$.

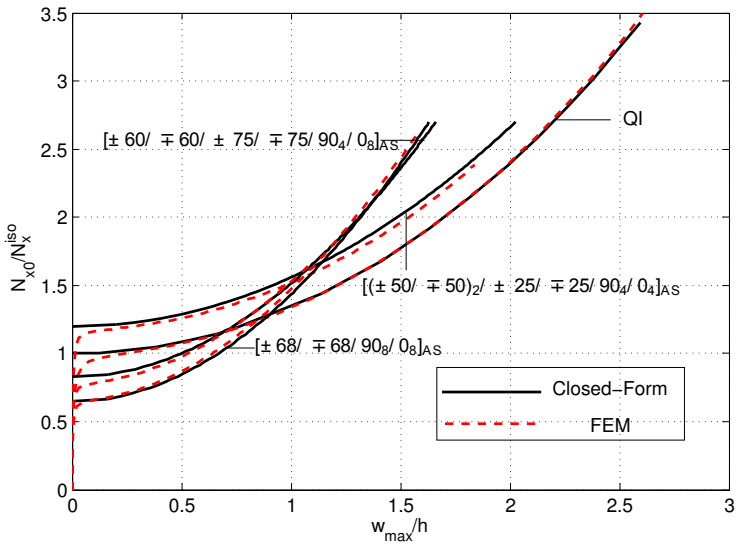

Fig. 4 Postbuckling responses of the optimal layups of a square plate under uniaxial compression for minimizing the maximum transverse deflection: Normalised axial loads N_x/N_x^{iso} versus Normalized maximum transverse displacement w_{max}/h function.

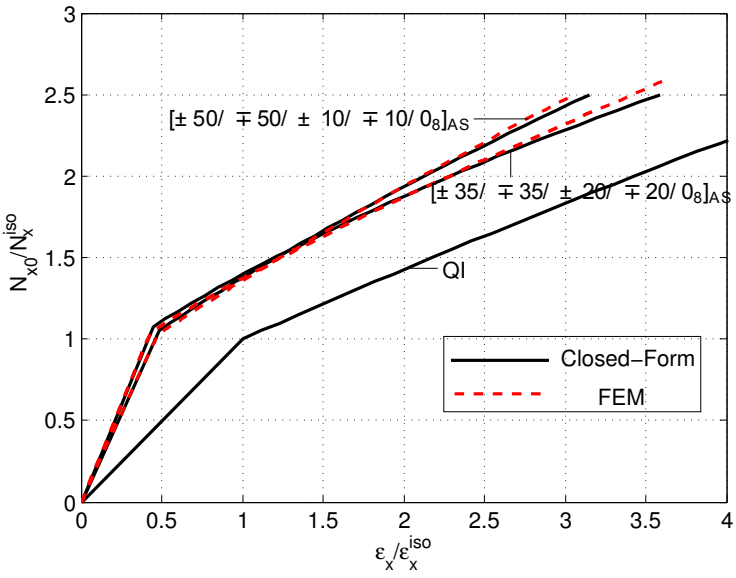

Fig. 5 Postbuckling responses of the optimal layups of a square plate under biaxial compression ($k = 0.2$) for minimizing the end-shortening strain: Normalised axial loads N_x/N_x^{iso} versus Normalised axial strain $\epsilon_x/\epsilon_x^{iso}$.

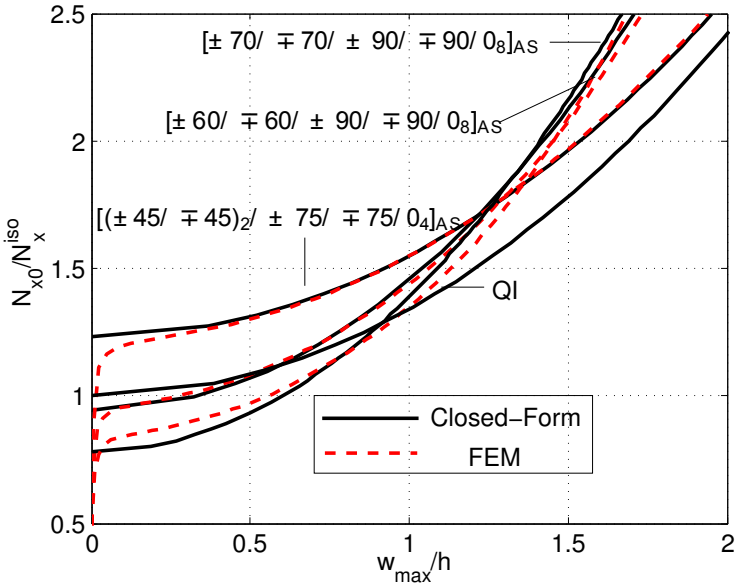

Fig. 6 Postbuckling responses of the optimal layups of a square plate under biaxial compression ($k = 0.2$) for minimizing the maximum transverse deflection: Normalised axial loads N_x/N_x^{iso} versus Normalized maximum transverse displacement w_{max}/h function.